Orientational Transitions in Symmetric Diblock Copolymers on Rough Surfaces

Yoav Tsori

Department of Chemical Engineering, Ben Gurion University, Beer Sheva 84105, Israel, and UMR 168 CNRS/Institut Curie, 11 rue Pierre et Marie Curie, 75231 Paris CEDEX 05, France

Easan Sivaniah

Department of Chemical Engineering, Texas Technical University, Lubbock, Texas 79409-3121

David Andelman*

School of Physics and Astronomy, Raymond and Beverly Sackler Faculty of Exact Sciences, Tel Aviv University, Tel Aviv 69978, Israel

Takeji Hashimoto

Department of Polymer Chemistry, Graduate School of Engineering, Kyoto University, Katsura, Kyoto 615-8510, Japan

As self-assembling systems become better understood, more emphasis is being given to finding ways to control the assembled structure, i.e., to orient ordered phases in a certain direction or anneal defects.[1−3] Block copolymers (BCP) are excellent model systems, which provide a good balance between price and chemical versatility, and are being extensively studied for technological applications as well as from a basic scientific viewpoint.[4−6] There are numerous ways to affect the BCP phase behavior and orientation, for example, using shear flow,[7] confinement between two solid chemically patterned surfaces,[8−15] or application of an external electric field.[16−20]

In this Note we consider a lamellar phase of symmetric diblock copolymers (the volume fraction of each monomer is $f = 0.5$) on top of a rough surface. The amplitude and periodicity of surface modulations determine whether the lamellae will be parallel or perpendicular to the substrate,[21,22] as has been recently shown experimentally by Sivaniah et al.[23,24] This new and alternative method to orient BCPs can be advantageous to the methods mentioned above because of its simple experimental setup. The aim of this Note is to extend results of a previous theoretical modeling[25] showing its direct applicability to existing experimental findings[23,24] and possibly suggesting new ones.

The surface roughness is modeled by a single one-dimensional corrugation mode, whose height in the *z*-direction above an (x, y) reference plane is given by $h(x) = R \cos(q_s x)$. As is shown on Figure 1, q_s and R are the wavenumber and amplitude of the surface roughness, respectively. The BCP is put above the substrate in the half-space $z \geq h(x)$. In addition, γ_{AB} is the interfacial interaction (per unit area) between the A and B blocks in the polymer chain, $\delta = \gamma_{subs,A} - \gamma_{subs,B}$ is the surface tension difference between the substrate and the two types of polymer blocks, and $q_0 = 2\pi/D$ is the

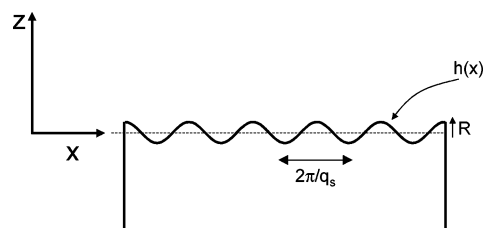* Corresponding author. E-mail: andelman@post.tau.ac.il.

Figure 1. Schematic illustration of the rough confining surface.

wavenumber of the bulk lamellae having a repeat period (ABBA) of size D.

We start by examining the order parameter of lamellae oriented perpendicular to the surface. The presentation follows the same lines as of ref 25:

$$\phi_\perp(\mathbf{r}) = \phi_0 \cos(q_0 x + q_0 u(x,z)) \qquad (1)$$

This is the deviation of the A-monomer relative concentration from its average value $f = 0.5$. The amplitude of sinusoidal variation, ϕ_0, depends on the degree of segregation and vanishes at the order−disorder temperature (ODT). The function $u(x,z)$ is a slowly varying function that describes surface-induced perturbations of the lamellae from their perfect shape. We write the bulk part of the free energy, in complete analogy with the elastic energy of smectic liquid crystals:[21,26]

$$F_b = \frac{1}{2} \int [K(u_{zz})^2 + B(u_x)^2] \, d^3r \qquad (2)$$

where $u_x = \partial u/\partial x$, $u_{zz} = \partial^2 u/\partial z^2$, $K \sim D\gamma_{AB}$ is the bending modulus, and $B \sim \gamma_{AB}/D$ is the compression modulus.

Several assumptions are made regarding the length scales and energies involved, as are explained in more detail in ref 25:

$$1 > q_0 R > q_s R > (q_0 R)^{3/2} \qquad (3)$$

and

$$\phi_0 \delta \ll \sqrt{BK} \simeq \gamma_{AB} \qquad (4)$$

We will be mainly interested in the poly(styrene)/poly(methyl methacrylate) system, where the A-block is chosen as the PS and the B-block as PMMA. The corresponding parameters are $\delta \simeq 0.25$ mN/m for the surfaces considered below and $\gamma_{AB} = 1$ mN/m, so eq 4 roughly holds. The inequalities in eq 3 are not satisfied in all the experiments. While $q_0 R$ is indeed larger than $q_s R$, $q_0 R$ is between 1 and 4 and is not smaller than unity as assumed. Therefore, $q_0 R > (q_0 R)^{3/2}$ does not strictly hold. Nevertheless, using the above inequalities, we were able to make simple analytical predictions by minimizing the energy with respect to the distortion field u. Up to numerical prefactors, the bulk free energy of the perpendicular state is[25]

$$\frac{F_\perp^0}{S} \sim \frac{\delta^2 \phi_0^2}{K} \frac{1}{q_0} \qquad (5)$$

where S is the surface area.

Table 1. Experimental Results from Ref 24 for Different PS/PMMA Samples and Different Rough Surfaces[a]

surface	q_s [nm^{-1}]	R [nm]	18K−18K $q_0 = 0.22$ nm^{-1}, $D = 28.6$ nm	38K−36.8K $q_0 = 0.17$ nm^{-1}, $D = 36.7$ nm	50K−54K $q_0 = 0.14$ nm^{-1}, $D = 43.5$ nm
rough SC-ITO	0.04	14.5	perp	perp	perp
rough UC-ITO	0.04	8		para	
smooth S-ITO	0.016	3.2		para	
rough SC-PIM	0.04	14.5		perp	

[a] Left column indicates the type of substrate used; q_s and R are the corrugation wavenumber and amplitude, respectively (see also Figure 1). The name of a sample indicates the molecular weight of the PS/PMMA blocks. The morphology is given for the six experiments that were carried out.

We repeat the same calculation as above but now for parallel lamellae. The order parameter is given by

$$\phi_\parallel(\mathbf{r}) = -\phi_0 \cos(q_0 z + q_0 u(x,z)) \qquad (6)$$

and the bulk free energy is

$$F_b = \frac{1}{2}\int [K(u_{xx})^2 + B(u_z)^2]\, \mathrm{d}^3 r \qquad (7)$$

We minimize the distortion field u in the same limits as in eqs 3 and 4 and find[25]

$$\frac{F_\parallel^0}{S} \sim \frac{\delta^2 \phi_0^{\,2}}{K}\frac{1}{q_0}\left(\frac{q_0}{q_s}\right)^2 (q_0 R)^2 \qquad (8)$$

Equations 5 and 8 use the surface energy to obtain the distortion field u. We now add this substrate−BCP interfacial tension and compare the gain and loss in the total free energy of the two states, including the bulk distortion and interfacial tension terms. This was not done in ref 25. In the case of perpendicular lamellae, the substrate is approximately equally covered by the A- and B-monomers (the symmetric case of PS/PMMA). Hence, adding the interfacial tension term to eq 5 results in the following free energy:

$$\frac{F_\perp}{S} \simeq \frac{\delta^2 \phi_0^{\,2}}{K}\frac{1}{q_0} + \frac{1}{2}(\gamma_{\text{subs,A}} + \gamma_{\text{subs,B}})\left(1 + \frac{1}{4}(q_s R)^2\right) \qquad (9)$$

The extra factor $1 + \frac{1}{4}(q_s R)^2$ is the ratio between the real surface profile $h(x) = R\cos(q_s x)$ and the flat one, $h = 0$, for small surface corrugations.

For parallel lamellae, we have a surface in contact with a layer rich in B-monomers (PMMA). Neglecting surface proximity effects, we consider that this layer has a concentration of B-monomer with amplitude $\frac{1}{2} - \phi_0$ and A-monomers (PS) with amplitude $\frac{1}{2} + \phi_0$, recalling that ϕ_0 is the deviation of the order parameter from $\frac{1}{2}$. The energy is $(\frac{1}{2} - \phi_0)\gamma_{\text{subs,A}} + (\frac{1}{2} + \phi_0)\gamma_{\text{subs,B}}$, and the total parallel free energy becomes

$$\frac{F_\parallel}{S} \simeq \frac{\delta^2 \phi_0^{\,2}}{K}\frac{1}{q_0}\left(\frac{q_0}{q_s}\right)^2 (q_0 R)^2 +$$
$$\left[\left(\frac{1}{2} - \phi_0\right)\gamma_{\text{subs,A}} + \left(\frac{1}{2} + \phi_0\right)\gamma_{\text{subs,B}}\right]\left(1 + \frac{1}{4}(q_s R)^2\right) \qquad (10)$$

To find the orientation transition, we equate $F_\parallel$ to $F_\perp$ (eqs 9 and 10) while estimating $Kq_0 \simeq 2\pi\gamma_{\text{AB}}$. The transition value of $(q_s R)^2$ is given by

$$(q_s R)^2 = \frac{\phi_0 \delta + 2\pi\gamma_{\text{AB}}}{\phi_0\delta(q_0/q_s)^4 - \frac{\pi}{2}\gamma_{\text{AB}}} \qquad (11)$$

Note that this equation includes the information on the melt segregation via ϕ_0 ($|\phi_0| < \frac{1}{2}$). Naturally, as the temperature approaches the ODT, ϕ_0 tends to zero, and the energetic difference between the parallel and perpendicular states goes to zero as well.

To compare these predictions of the lamellar orientation dependence on the various roughness parameters, we used some of the results reported in ref 24. In that paper sample orientation was determined by a combination of cross-sectional TEM microscopy, atomic force microscopy, and dynamic secondary-ion mass spectroscopy. The principle result was to demonstrate that an increase in the substrate roughness amplitude, R, led to a transition from parallel to perpendicular orientation, while other substrate parameters were untouched. The χN values of the samples vary between 10.8 and 30 and, thus, are in the weak to intermediate segregation regimes, where the predictions of our model can be applied. For strongly segregated block copolymers the derivation given above can be qualitatively applied but is of less accuracy.

In ref 24 the temporal evolutions of several BCP systems showing different equilibrium orientations have been investigated. We have chosen only six systems where the equilibrium perpendicular or parallel orientations have been thoroughly verified. They include three molecular weights of symmetric PS−PMMA block copolymer (of different q_0) on four substrates of different q_s. We can use these observations to test the validity of our current theoretical model. The BCP samples are denoted 18K−18K, 38K−36.8K, and 50K−54K, according to the molecular weight of PS and PMMA blocks in the chain, respectively. The four substrates are super-critically rough indium tin oxide (SC-ITO), under-critically rough ITO (UC-ITO), smooth ITO (S-ITO), and super-critically rough polyimide (SC-PIM). All the experimental parameters are summarized in Table 1. The prefixes of *super-* and *under-* were used to denote the degree of roughness of the substrates. The SC-PIM substrate was made by imprinting a polyimide surface with a SC-ITO surface. Therefore, SC-PIM and SC-ITO had identical topological features. Contact angle measurements at 200 °C on all of the substrates revealed that there was no large difference in the wetting properties of PS and PMMA on all of these substrates. For more details see ref 24.

An assumption of identical substrate surface energy allows all six observations to be collated onto a single orientational phase diagram. In Figure 2 we plot the experimental points and the transition lines predicted by eq 11 on three types of plots. In part a, $q_0 = 2\pi/D$ is used to scale the two other parameters: q_s and R and to produce two dimensionless parameters for the plot: q_s/q_0 and $q_s R$. In the range of experimental parameters, the transition line between parallel and perpendicular states, eq 11, is very close to a straight line (up to about
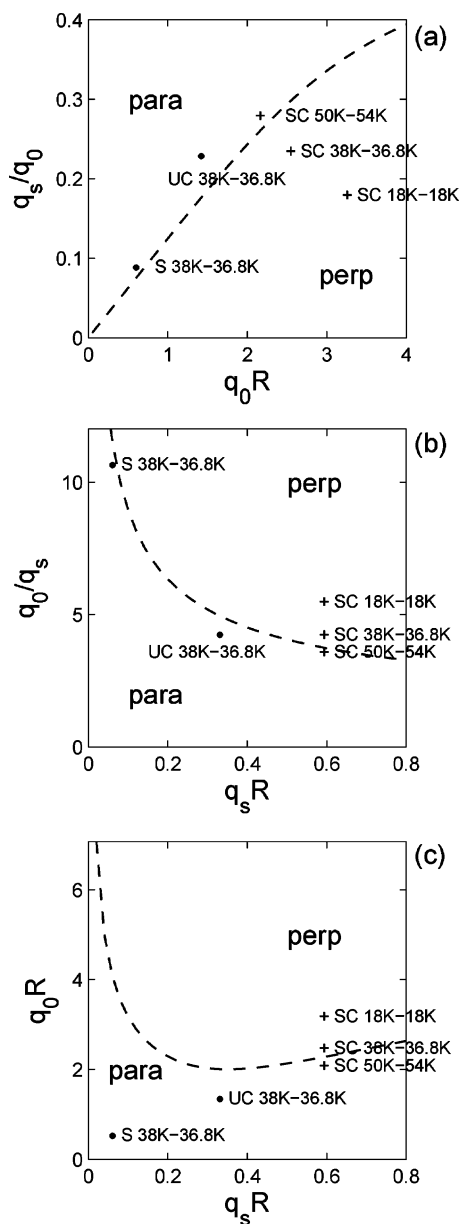
Figure 2. Comparison between the model and experimental phase diagram for the perpendicular and parallel lamellar configurations on a rough substrate. The dashed line is calculated from eq 11. (a) R and q_s are scaled by q_0, the lamellae wavenumber. The "+" data points correspond to observed perpendicular morphology, while the "•" ones to parallel lamellae (see also Table 1). (b) A different plot of the same theoretical prediction from eq 11 and experimental points. The surface wavenumber q_s is used to scale q_0 and R. (c) The surface amplitude R is used to scale q_0 and q_s. In all three plots $\gamma_{AB} = 1$ mN/m, $\delta = 0.25$ mN/M, and $\phi_0 = 0.4$.

$q_0 R \simeq 2.5$ in Figure 2a). Namely, for a fixed q_0, $q_s \sim R$.

Figure 2a shows that all samples found to be in the parallel morphologies in the experiments lie indeed above the theoretical transition line and all perpendicular morphologies lie below it, with the exception of the SC-ITO 50K−54K sample, which lies a little inside the parallel region, although it is measured as a perpendicular state.

The same information is presented differently in parts b and c of Figure 2. In (b) we think of q_s as the rescaling factor and plot q_0/q_s as a function of $q_s R$. From eq 11 and under the condition $\gamma_{AB} \ll \phi_0\delta$, we get $q_0/q_s \simeq (q_s R)^{-1/2}$. In Figure 2b we see again that, besides the

SC-ITO 50K−54K sample, all other data points fit with the theoretical prediction. And finally in Figure 2c, q_0 and q_s are rescaled by R.

The phase diagrams in parts b and c may seem counter-intuitive at first sight. At a given surface roughness $q_s R$, the transition from the parallel phase to the perpendicular one occurs as D decreases (or q_0 increases). This surprising behavior can be understood by looking at the dependence of the distortion field $u(x,z)$ on the distance z from the surface. For perpendicular lamellae, $u \sim \exp(-k_\perp z)$, where $k_\perp \sim 1/D$. Hence, distortions relax at a distance from the substrate comparable to the lamellar spacing. Undulations in the parallel phase, however, are given by $u \sim \exp(-k_\| z)$, where $k_\| = q_s^2/q_0$. As the BCP molecular weight decreases, D decreases, $q_0 \sim D^{-1}$ increases, and $k_\| \sim D$ decreases, resulting in a longer extent of the distortion u field in the z direction. Hence, the accumulated frustration of parallel lamellae leads to their relative instability toward the perpendicular phase. In other words, the smaller the molecular weight is, the more stable the perpendicular lamellae tend to be.

In a different interpretation of the same experimental data,[24] it was inferred that the transition between parallel and perpendicular lamellae is expected to be at $q_s R \sim 1$ and independent of q_0. Using the values of $\delta = 0.25$ mN/M and $\gamma_{AB} = 1$ mN/M the prefactor is very close to unity, yielding $q_s R \simeq 0.98$. This result is based on a previous calculation,[21] which gave the energy of parallel lamellae (in the strong segregation regime) as $\sim(q_s R)^2$. These two theoretical fits are based on different assumptions and would look quite different if plotted on Figure 2. However, because of the limited number of experimental systems, it is hard to rule out any of the two theoretical fits.

In summary, we propose a simple model to interpret the orientation transition seen in BCP systems in contact with rough substrates. More experiments should be carried out in order to fully map the phase diagram. In particular, special attention should be given to the possible creation of island and holes or other defects which are not included in the present theoretical framework.

References and Notes

(1) Park, C.; Yoon, J.; Thomas, E. L. *Polymer* **2003**, *44*, 6725.
(2) Grier, D. G. *Nature (London)* **2003**, *424*, 810. Dufresne, E. R.; Grier, D. G. *Rev. Sci. Instrum.* **1998**, *69*, 1974.
(3) Lyuksyutov, S. F.; Vaia, R. A.; Paramonov, P. B.; Juhl, S.; Waterhouse, L.; Ralich, R. M.; Sigalov, G.; Sancaktar, E. *Nat. Mater.* **2003**, *2*, 468.
(4) Leibler, L. *Macromolecules* **1980**, *13*, 1602. Ohta, T.; Kawasaki, K. *Macromolecules* **1986**, *19*, 2621.
(5) Matsen, M. W.; Schick, M. *Phys. Rev. Lett.* **1994**, *72*, 2660.
(6) Matsen, M. W.; Bates, F. S. *Macromolecules* **1996**, *29*, 1091.
(7) Riise, B. L.; Fredrickson, G. H.; Larson, R. G.; Pearson, D. S. *Macromolecules* **1995**, *28*, 7653. Koppi, K. A.; Tirrell, M.; Bates, F. *Phys. Rev. Lett.* **1993**, *70*, 1449.
(8) Turner, M. S. *Phys. Rev. Lett.* **1992**, *69*, 1788.
(9) Turner, M. S.; Rubinstein, M.; Marques, C. M. *Macromolecules* **1994**, *27*, 4986.

(10) Turner, M. S.; Maaloum, M.; Ausserré, D.; Joanny, J.-F.; Kunz, M. *J. Phys. II (France)* **1994**, *4*, 689.

(11) Li, Z.; Qu, S.; Rafailovich, M. H.; Sokolov, J.; Tolan, M.; Turner, M. S.; Wang, J.; Schwarz, S. A.; Lorenz, H.; Kotthaus, J. P. *Macromolecules* **1997**, *30*, 8410.

(12) Petera, D.; Muthukumar, M. *J. Chem. Phys.* **1998**, *109*, 5101.

(13) Tsori, Y.; Andelman, D. *J. Chem. Phys.* **2001**, *115*, 1970. Tsori, Y.; Andelman, D. *Eur. Phys. J. E* **2001**, *5*, 605.

(14) Mansky, P.; Russell, T. P.; Hawker, C. J.; Mayes, J.; Cook, D. C.; Satija, S. K. *Phys. Rev. Lett.* **1997**, *79*, 237.

(15) Wang, Q.; Yan, Q.; Nealey, P. F.; de Pablo, J. J. *J. Chem. Phys.* **2000**, *112*, 450.

(16) Amundson, K.; Helfand, E.; Quan, X.; Smith, S. D. *Macromolecules* **1993**, *26*, 2698.

(17) Thurn-Albrecht, T.; Schotter, J.; Kästle, G. A.; Emley, N.; Shibauchi, T.; Krusin-Elbaum, L.; Guarini, K.; Black, C. T.; Tuominen, M. T.; Russell, T. P. *Science* **2000**, *290*, 2126.

(18) Böker, A.; Knoll, A.; Elbs, H.; Abetz, V.; Müller, A. H. E.; Krausch, G. *Macromolecules* **2002**, *35*, 1319.

(19) Ashok, B.; Muthukumar, M.; Russell, T. P. *J. Chem. Phys.* **2001**, *115*, 1559. Pereira, G. G.; Williams, D. R. M. *Macromolecules* **1999**, *32*, 8115. Tsori, Y.; Andelman, D. *Macromolecules* **2002**, *35*, 5161.

(20) Tsori, Y.; Tournilhac, F.; Andelman, D.; Leibler, L. *Phys. Rev. Lett.* **2003**, *90*, 145504. Tsori, Y.; Tournilhac, F.; Leibler, L. *Macromolecules* **2003**, *36*, 5873.

(21) Turner, M. S.; Joanny, J.-F. *Macromolecules* **1992**, *25*, 6681.

(22) Podariu, L.; Chakrabarti, A. *J. Chem. Phys.* **2000**, *113*, 6423.

(23) Sivaniah, E.; Hayashi, Y.; Iino, M.; Hashimoto, T.; Fukunaga, K. *Macromolecules* **2003**, *36*, 5894.

(24) Sivaniah, E.; Hayashi, Y.; Matsubara, S.; Kiyono, S.; Hashimoto, T.; Fukunaga, K.; Kramer, E. J.; Mates, T. *Macromolecules* **2005**, *38*, 1837.

(25) Tsori, Y.; Andelman, D. *Macromolecules* **2003**, *36*, 8560.

(26) de Gennes, P. G.; Prost, J. *The Physics of Liquid Crystals*, 2nd ed.; Oxford University Press: Oxford, 1993.